



# Stratigraphy and hydrology of a subpolar ice field, King George Island

J.M. Travassos<sup>(†)</sup>, J.C. Simões<sup>(‡)</sup>

<sup>(†)</sup> CNPq-Observatório Nacional, Brasil.

<sup>(‡)</sup> Inst. Geociências, Univ. Federal do Rio Grande do Sul, Brasil.

## Abstract

A GPR survey was carried out to study the ice structure and hydrology at the main dome of the King George Island ice field, Antarctica. The transmitted wavelets bandwidth was centered at 50MHz. Data show the presence of free water in snow and in ice fractures. The water signature was inferred from the wavelet phase. A nearby borehole allowed the calibration of the GPR sections in terms of composition and of resolving power of ice layers. Broadside perpendicular and parallel antenna data collection schemes allowed for the identification of crevasses in the area.

## INTRODUCTION

The GPR technique has been a common tool for the exploration of cold regions due to the excellent penetration of radio waves in ice and frozen ground. This is because in contrast to most materials, cold ice is relatively transparent to radar waves. In fact, radio echo devices and radar systems have been developed for a variety of large-scale applications in Glaciology over the last three decades. Deep penetrating radar have been used to map the bedrock beneath glaciers and ice sheets to depths as great as several kilometers (e.g. Bogorodsky et al., 1985). Those systems are operated on the ice surface or are airborne. Radar systems operating from aircraft suffer from the strong reflection at the air-ground interface that dramatically reduces the amount of energy entering the ice and thus the depth of penetration (Arcone et al., 1995).

GPR have been used in Glaciology to produce ice stratigraphy (Arcone, 1996; Murray et al., 1997), to determine accumulation rates by interpreting reflecting horizons in Antarctic firn (Forster et al., 1991), and on temperate glaciers (Holmlund and Richardson, 1995; Kohler et al., 1997). In addition, GPR can also be used for inferring the dielectric properties of near-surface snow, firn and ice that are important for interpreting SAR satellite images (Rott et al., 1993).

In this work we study the structure and composition of ice as revealed by GPR images at the top of the King George Island ice field (above 600 m of altitude). Those images are calibrated with the results from a nearby borehole. Previous study demonstrated that the ice cover at the dome should be thicker than 300 m (Macheret et al., 1996). The present study were part of a larger survey investigating the mass balance of Lange Glacier (62° 7' S, 58 36' W), an outlet glacier that has receded about 1 km since 1956, probably due to region warming (Aquino, 1999). Average temperature at King George Island has risen 0.98 °C from 1947 to 1995 (Aquino, 1999). Ice at the study site is near the pressure melting point.

## EQUIPMENT AND FIELD PROCEDURES

The radar system was composed of a PULSE EKKO IV and bi-static unshielded 50 MHz antennae with a 50 MHz pulse bandwidth. We have used a 100 V pulser with a 6 ns rise time, best suited to the low frequency antenna. The antennae were dragged by hand in both broadside perpendicular (BPer) and parallel (BPar) configurations and kept 2 m apart for the common-offset reflection profiles. The velocity was estimated via a CMP profile. Ground coupling problems were kept to a minimum due to the step-by-step way the antennae were dragged along the profiles.

Theoretical transmit directivities and footprint for an unshielded, finite-size loaded dipole operating monostatically on a homogeneous half-space of ice are useful to understand the GPR images obtained in this work. Those radiation patterns can be easily found in the literature (Arcone, 1995). For the purposes of this work it is important to keep in mind that the radiation pattern on the H-field plane, a vertical plane perpendicular to the antenna axis, has maximum intensity in two shell-like lobes. This makes the footprint along the profile direction of a broadside perpendicular configuration roughly twice as long as in the perpendicular direction at any given depth (Arcone, 1995). This footprint pattern indicates that sensitivity is greater along the H-field plane. Footprint pattern associated with the cone of irradiated energy (which has apertures well above 90°) indicates that diffractions in ice can have asymptotes with higher signal strengths than their apexes. Conversely, a BPar configuration will be less sensitive to diffractions within the ice.

Field data was collected along three profiles as shown in Fig. 1. Profiles were 50-80 m long. Data was collected with a time window of 2040 ns and a sampling rate of 1.6 ns. The adopted step size was 0.5 m for the common offset and 0.2 m for the CMP schemes. Those profiles were done to provide a standard as well as to calibrate the larger Lange Glacier survey. A relatively high stack of 16 was used throughout. A total of 6 GPR profiles were obtained along the field layout shown in Fig. 1. Antenna configuration varies between profiles. Table 1 shows how the profiles were done in respect to direction, antenna configuration and type.

Profile	Direction	Ant. Conf.	Type
P01	AB	BPer	R
P02	AB	BPar	R
P03	AC	BPar	R
P04	AC	BPer	R
P05	AD	BPer	R
P06	AB	BPer	C

**Table 1.** GPR profile direction, antenna configuration and type. BPer is broadside perpendicular, BPar is broadside parallel, R stands for reflection line and C for a CMP line.

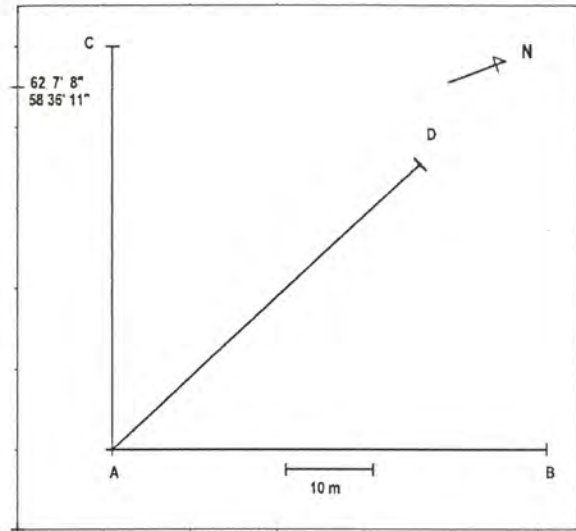


**Figure 1.** Field layout for the GPR profiles. The location of the survey is given at the mark on the upper left corner.

Profile P06 was used to infer a phase velocity in the ice. A velocity analysis was performed stacking after moveout correction, using a stretch of 10%. The estimated velocity in the studied area was  $V_{ice} = 0.19$  m/ns. This relatively high value was later confirmed by observing the migrated results of the common-offset sections. Note that this value is 19% higher than the tabulated velocity of ice: 0.16 m/ns.

#### WELL LOG DATA AND RESOLUTION

This paper uses the results from a 49,7 m long ice core drilled one year before, at about 2.5 km SW of the surveyed area. Results allow us to estimate a minimum detectable thickness in the GPR sections. The vertical resolution of the GPR data is determined by the bandwidth center frequency wavelength. For the 50 MHz configuration used here, and for the estimated phase velocity of the electromagnetic field in the glacier, the practical wavelength is  $\lambda = 3.8$  m. The level of detectability of a given ice horizon will be a function of that wavelength.

The ice core revealed a high number of thin layers ranging from 1 mm wind crusts to 4 cm ice layers. Somewhat thicker layers of 6-20 cm were also found in some sections. Coarse grain layers, thicker than 1.15 m, thick are also reported. The question here is to assess whether thin stratigraphic horizons, like the ones observed in the core, are detectable with the GPR wavelet. The power to detect a thin bed will depend on the ability to distinguish between the properties of two layers, which in turn also depends on the signal-to-noise ratio. As the layers become thinner, the reflected energy becomes a composite of the reflections on both interfaces. Less and less independent information from the two interfaces is available. But the two reflections combine in a way that there is still enough energy to detect the layer, although it is not possible to resolve its thickness  $b$ . The lower limit is  $b = \lambda/8$ , in the absence of noise. In that case the only information that is left is a combination of the two reflections (Widess, 1973). Even beds as thin as  $b = \lambda/20$  should be detectable with an amplitude about 60% of a thick bed at the same depth (Widess, 1973). On the other hand destructive interference can render a not so thin layer of  $b = \lambda/2$ , just under 2 m, transparent to radar (Rossiter et al, 1975; Widess, 1973). A theoretically detectable thin bed in this work falls in the range  $b = [0.02, 0.48]$  m. Density measurements were done at each 11 cm along the ice core. This allows for resolving the density of a given layer if it is at least 22 cm thick. In terms of density measurements about 34% of the recognizable layers in the ice core fall in the category of a thin layer, i.e., between 22 and 48 cm. Thick layers account for 8% of the total.

Comparison of GPR and ice core data can be done estimating an averaged trace. We show this by estimating the average trace of profile P02, chosen because its antenna configuration BPar because it is insensitive to the top of the crevasses in the area. Other profiles, e.g., profile P01, displays diffractions associated to the top of crevasses. A main body of water was found in the borehole about 37 m deep. The water occurs within a coarse grain firn level about 1 m thick. P02 detects the water table at 32.5 m. This discrepancy is consistent with the difference in height between the surveyed area and the borehole. Fig. 2 shows the averaged trace of P02, with a spreading exponential compensation gain and maximum amplitude normalized to 1. The same figure displays the observed values of ice densities as obtained

from the core measurements. Depths for the averaged trace are estimated for a velocity of 0.19 m/ns. Note that the transition between firn and ice occurs at the density of 0.830 g/cm<sup>3</sup>.

## GPR PROFILES

The strongest signal in all reflection profiles is due to the water table level below 32 m, dividing the sections in two parts. Sections show strong near-surface reflectors sitting on weaker reflectors above the water table. Below the water table reflectors become stronger again, displaying many discrete events that reach the end of the sections. An important distinction between profiles is given by the different responses of the two antenna configurations. Profiles done with the BPer configuration detect the top of crevasses buried under the snow cover producing a crisscrossing pattern due the interference of closely spaced diffractions. This pattern is easily cleared out by collapsing the diffractions via a single-velocity migration. Only subtle indication of crevasses is left after migration, indicating that they are almost transparent but for their top sections. Profiles done with BPar configuration are a great deal less sensible to crevasses, displaying a similar picture to the migrated BPer profiles. Probably the main signature of a crevasse in the area comes from the bottom of the snow bridge covering it.

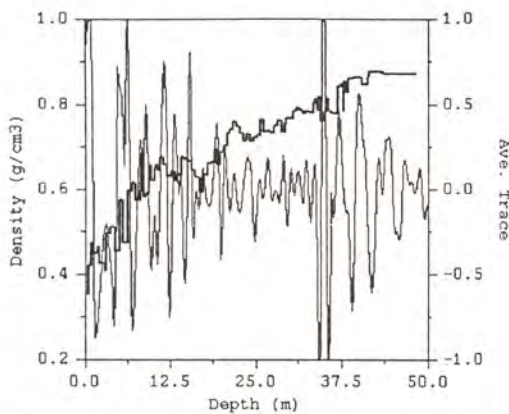


**Figure 2.** Density log and averaged trace of profile P02. The strong reflection below 32 m corresponds to the top of the water table.

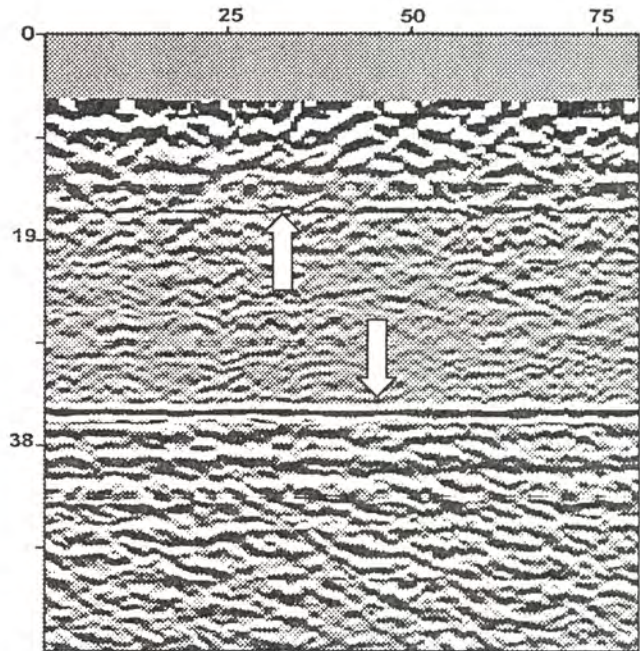


**Figure 3.** First 60m of profile P02. The arrows show two water table levels. The downward arrow points to the main water body. The direct arrivals on the top of the section are muted. Depths and distances are in meters.

Figure 3 shows the first 60 m of the profile P02 section. The reflection of the water table is marked with a downward arrow. Another water level at about 16 m, revealed by a similar phase inversion, is indicated by the upward arrow. Several other levels are observed in that section. Subvertical reflectors are a common feature below the water table, probably indicating plastic deformation patterns in the ice. The transition firn-ice occurs below the water table as it should be expected. Another important feature is a crevasse vertical signature just before 25 m from the beginning of the profile, easily observed as a pull down of reflections between the two water levels. Apparently, this crevasse is a feeding channel for the water table, as indicated by the phase shifts along its way. There are evidences of a few other crevasses, suggesting a drainage system communication between the upper and lower water levels as well as to greater depths.

## CONCLUSIONS

GPR profiles were used to identify the thickness and lateral extent of some ice structures. The maximum depth observed in the GPR profiles is 195 m, well short of the estimated local ice thickness (> 300 m). A nearby borehole was used to help understanding the reflections seen in the GPR sections. The low noise level in the area results in clear reflections from layers of a wavelength fraction thick, allowing the correlation of horizons with the ice core. The strongest reflections within the ice result from the free water in the glacier; they are accompanied by a clear change in wavelet phase. The presence of crevasses, ubiquitous in the survey area as revealed by the diffractions, originated mostly at the bottom of the snow bridges. Diffractions were minimized either by migration of BPer profiles, or by restricting to the BPar profiles. The

two resulting sections display an equivalent degree of resolution rendering similar complexity for the ice field. Some crevasse signatures indicate that they play an important role in the glacier water drainage system.

## REFERENCES

- Aquino, F.E. 1999, Sedimentação moderna associada à Geleira de Maré Lange. MSc dissertation, Rio Grande do Sul Federal University, Institute of Geosciences, 106 pp.
- Arcone, S.A., 1996. High resolution of glacial ice stratigraphy: a ground-penetrating radar study of Pegasus Runway, Mc Murdo Station, Antarctica, *Geophys.*, 61: 1653-1663.
- Arcone, S.A., D.E. Lawson and A.J. Delaney, 1995, Short-pulse radar wavelet recovery and resolution of dielectric contrasts within englacial and basal ice of Matanuska Glacier, Alaska, U.S.A. *Journal of Glaciology*, vol. 41, pp. 68-86.
- Arcone, S.A., 1995, Numerical studies of the radiation patterns of resistively loaded dipoles, *J. App. Geophys.*, 33, 39-52.
- Bogorodsky, V.V., C.R. Bentley and P.E. Gudmandsen, 1985, *Radioglaciology*, D. Reidel, Dordrecht, Netherlands, 1985.
- Forster, R., C. Davis, T. Rand, and R.K. Moore, 1991, Snow-stratification investigation on an Antarctic ice stream with an X-band radar system. *Journal of Glaciology.*, 37(127), 323-325.
- Kohler, J., Moore, J.C., Kennett, M., Engeset, R., and Elvehoy, H., 1997, Using ground-penetrating radar to image previous years' summer surfaces for mass-balance measurements, *Annals of Glaciology*, 24, 355-360.
- Macheret, Y.Y., Moskalevsky, M.Y., Simoes, J.C., Ladouch, L., 1996. Study of King George Island ice cap, South Sheatland Islands, Antarctica, using radio-echo sounding and spot ERS-1 SAR Satellite images, *Proc. Int. Seminar on the Use and Application of ERS in Latin America*, Vina del Mar, Chile, 25-29.
- Murray, T., D.L. Gooch and G.W. Stuart, 1997, Structures within the surge front at Bakaninbreen, Svalbard, using ground-penetrating radar, *Annals of Glaciology*, 24, 122-129.
- Rott, H., K. Sturm and H. Miller, 1993, Active and passive microwave signatures of Antarctic firn by means of field measurements and satellite data. *Annals of Glaciology*, 17, 337-343.
- Rossiter, J.R., D.W. Strangway, A.P. Annan, R.D. Watts, J.D. Redman, 1975, Detection of thin layers by radio interferometry, *Geophys.*, 40, 299-308.
- Widess, M.B., 1973, How thin is a thin bed?, *Geophys.*, 38, 1176-1180.

## ACKNOWLEDGMENTS

Funding for this research was provided by the Brazilian Antarctic Program (PROANTAR) and the Brazilian National Council for Scientific and Technological Development (CNPq). JMT and JCS were supported by CNPq grants.